REPORT DOCUMENTATION PAGE

Form Approved
OMB No. 0704-0188

PLEASE DO NOT RETURN YOUR FORM TO THE ABOVE ORGANIZATION.

1. REPORT DATE *(DD-MM-YYYY)*	2. REPORT TYPE	3. DATES COVERED *(From - To)*
09-02-2012	FINAL	01-03-2009-30-11-2011

4. TITLE AND SUBTITLE
Nonlinear Wave Propagation

5a. CONTRACT NUMBER

5b. GRANT NUMBER
FA9550-09-1-0250

5c. PROGRAM ELEMENT NUMBER

6. AUTHOR(S)
Mark J. Ablowitz

5d. PROJECT NUMBER

5e. TASK NUMBER

5f. WORK UNIT NUMBER

7. PERFORMING ORGANIZATION NAME(S) AND ADDRESS(ES)
University of Colorado

8. PERFORMING ORGANIZATION REPORT NUMBER

9. SPONSORING/MONITORING AGENCY NAME(S) AND ADDRESS(ES)
Air Force Office of Scientific Research
875 North Randolph Street
Suite 325, Rm 3112
Arlington, VA 22203
Dr. Arje Nachman/RSE

10. SPONSOR/MONITOR'S ACRONYM(S)

11. SPONSOR/MONITOR'S REPORT NUMBER(S)
AFRL-OSR-VA-TR-2012-1166

12. DISTRIBUTION/AVAILABILITY STATEMENT
Distribution A: Approved for public release

13. SUPPLEMENTARY NOTES

14. ABSTRACT

The PI's research program in nonlinear wave propagation is broad based and very active. There have been a number of important research contributions carried out as part of the effort funded by the Air Force. During the period 1 March 2009 -- 30 November 2011, fourteen papers were published in refereed journals,. In addition one refereed book and one refereed conference proceeding were published and thirty one invited lectures were given. The key results and research directions are described in the final report. Full details can be found in our research papers which are also listed at the end of this report. New models of mode-locked lasers were developed and studied. Investigations of nonlinear waves in photonic lattices led to new mathematical models which explain experimental observations. New results associated with dark solitons were obtained and applied to mode-locked lasers. Dispersive shock waves were analyzed and results compared favorably with experiments.

15. SUBJECT TERMS
Nonlinear wave propagation

16. SECURITY CLASSIFICATION OF:			17. LIMITATION OF ABSTRACT	18. NUMBER OF PAGES	19a. NAME OF RESPONSIBLE PERSON
a. REPORT	b. ABSTRACT	c. THIS PAGE			Mark J. Ablowitz
U	U	U	U		19b. TELEPHONE NUMBER *(Include area code)* 303-492-5502

Reset

Standard Form 298 (Rev. 8/98)
Prescribed by ANSI Std. Z39.18

Nonlinear Wave Propagation
AFOSR Grant/Contract # FA9550-09-1-0250
Final Report
1 March 2009 – 30 November 2011

9 February 2009

Mark J. Ablowitz
Department of Applied Mathematics
University of Colorado
Boulder, CO 80309-0526
Phone: 303-492-5502
Fax:303-492-4066
email address: mark.ablowitz@colorado.edu

OBJECTIVES

To carry out fundamental and wide ranging research investigations involving the nonlinear wave propagation which arise in physically significant systems with emphasis on nonlinear optics. The modeling and computational studies of wave phenomena in nonlinear optics include ultrashort pulse dynamics in mode-locked lasers, dynamics and perturbations of dark solitons, nonlinear wave propagation in photonic lattices, investigations of dispersive shock waves.

STATUS OF EFFORT

The PI's research program in nonlinear wave propagation is broad based and very active. There have been a number of important research contributions carried out as part of the effort funded by the Air Force. During the period 1 March 2009 – 30 November 2011, fourteen papers were published in refereed journals,. In addition, one refereed book and one refereed conference proceeding were published, and thirty one invited lectures were given. The key results and research directions are described below in the section on accomplishments/new findings. Full details can be found in our research papers which are listed at the end of this report.

Research investigations carried out by the PI and colleagues included the following. The underlying modes, dynamics and properties of mode-locked lasers which are used to create ultrashort pulses were analyzed. Titanium:sapphire (Ti:sapphire or Ti:s) lasers are often used to produce ultrashort pulses on the order of a few femtoseconds. There are other mode-locked lasers which produce ultrashort pulses, such as Sr-Forsterite, fiber lasers, and Chromium-doped lasers. Ti:s lasers are known to have outstanding characteristics. These mode-locked lasers can be used to generate a regularly spaced train of ultrashort pulses separated by one cavity round-trip time. A typical mode-locked laser system consists of a Ti:sapphire crystal which exhibits a nonlinear Kerr response and has a large normal group-velocity dispersion (GVD). This requires a set of prisms and/or mirrors specially designed to have large anomalous GVD in order to compensate for the normal GVD of the crystal. Experiments conducted at the University of Colorado with the mathematical foundation provided by our group, demonstrated that such lasers can be approximated by dispersion-managed systems and the intra-cavity pulse was found to be described by a dispersion-managed soliton.

Improved mathematical models of these mode-locked lasers containing gain and loss mechanisms were developed; these models contain gain and filtering terms saturated by energy and a loss term saturated by power. The new models describes the mode-locking and dynamics of localized nonlinear waves with/without dispersion management in both anomalous and normal regimes. Single and multi-soliton trains were obtained and analyzed.

Early experimental observation of one-dimensional nonlinear lattice modes in optical waveguide arrays demonstrated that at sufficiently high power, a laser beam could be self-trapped inside the waveguide. This demonstrated the formation of a lattice or discrete soliton. Importantly, such waveguides can be constructed on extremely small scales and they have been constructed by all-optical means. In turn, such nonlinear waves in waveguide arrays have attracted special attention due to their realizability.

Lattice nonlinear Schrödinger equations provide excellent models of photonic lattices. Investigations of the associated pulse propagation with special emphasis on lattices with background honeycomb structure was carried out. In the strong potential (i.e. strong background lattice) limit, sometimes called the tight binding limit, novel nonlinear discrete systems are obtained in a regime near special points, called Dirac points, associated with the underlying dispersion relation. In the continuous limit nonlinear Dirac systems are obtained. When the background lattice is weak a different types of Dirac systems are found.

We developed asymptotic and computational methods which describe perturbations to dark solitons in nonlinear Schrödinger type systems under perturbation. A fundamental feature that arises is the appearance of a shelf due which arises to the perturbation. The shelf is small but long in extent. Different perturbations can lead to prominent of relatively weak shelves. In ring dark soliton mode-locked laser systems the shelf can lead to substantial effects.

Dispersive shock waves (DSW's) were also investigated. Motivated by experiments at the University of Colorado, dispersive shock "blast" waves and interactions were studied. The relevant analytical approximations and theory for DSW's were developed and results were compared with experiment and computation. DSW's arise in nonlinear optics and many other areas of physics. Interactions of DSW's are not yet well understood; this is a topic of our current research.

ACCOMPLISHMENTS/NEW FINDINGS

Dynamics of ultra-short laser pulses and frequency combs

Research developments with mode-locked lasers, such as Ti:sapphire lasers, have enabled scientists to generate regularly spaced trains of ultrashort pulses, which are separated by one cavity round-trip time. Fig. 1 below shows a schematic of a mode-locked Ti:sapphire laser and the emitted pulse train. Typical values for a Ti:sapphire mode-locked laser are pulse width: $\tau = 10$ fs $= 10^{-14}$ sec and repetition time: $T_{\text{rep}} = 10$ ns $= 10^{-8}$ sec.

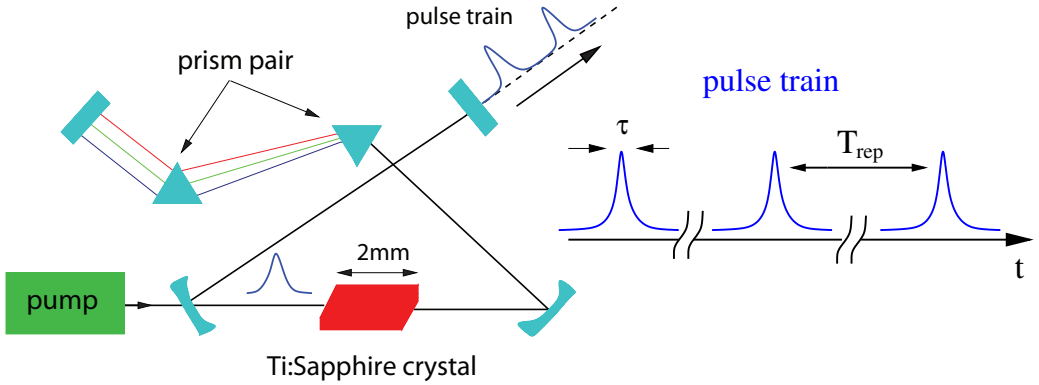

Figure 1: Ti:sapphire laser (left) and the emitted pulse train (right).

Associated with the spectrum, or the Fourier transform of the pulse train is a frequency comb, whose frequencies are separated by the laser's repetition frequency $f_{\text{rep}} = \frac{1}{T_{\text{rep}}} =$ 100 MHz. Progress in the development of optical oscillators has been made possible by controlling these femtosecond frequency combs. Extremely stable frequency combs have been generated by Ti:s laser systems, but other types of mode-locked lasers such as Sr:Forsterite and fiber lasers are also being studied intensively. We have been working with faculty in the Department of Physics at the University of Colorado who are leaders in this research effort. It is important to have useful mathematical models of these laser systems.

In our research we have been studying a distributed dispersion-managed equation which we term the power energy saturation (PES) model. For a pulse amplitude $u(z,t)$, power

$P(z,t) = |u|^2$, and energy $E(z) = \int_{-\infty}^{+\infty} |u|^2 \, \mathrm{d}t$, propagating in the z direction, the normalized or dimensionless equation we study takes the form

$$i\frac{\partial u}{\partial z} + \frac{d(z)}{2}\frac{\partial^2 u}{\partial t^2} + n(z)|u|^2 u = \frac{ig}{1 + E/E_{\text{sat}}}u + \frac{i\tau}{1 + E/E_{\text{sat}}}u_{tt} - \frac{il}{1 + P/P_{\text{sat}}}u \qquad (1)$$

where the constant parameters g, τ, l, E_{sat}, P_{sat} are positive. The first term on the right hand side represents saturable gain, the second is nonlinear filtering ($\tau \neq 0$) and the third is saturable loss. This model generalizes the well-known master laser equation originally developed by Haus and collaborators. When the loss term is approximated in the weakly-nonlinear regime by a first order Taylor polynomial we obtain the master laser equation. Hence, the master laser equation is included in the power saturated model as a first order approximation.

In our papers we discuss in detail how to get the above dimensionless system from the original dimensional variables. Briefly, the relationship between variables is given by

$$z' = z/z_*, t' = t/t_*, u = E/\sqrt{P_*}$$

where E is the envelope of the electromagnetic field t_*, P_* are the characteristic time (proportional to pulse width) and power respectively. We take $z_* = 1/(P_*\gamma_0)$, where γ_0 (in units 1/MW-mm) is the nonlinear coefficient in the laser crystal, g, τ and l are scaled by z_* and the normalized dispersion is given by $d(z) = -k''(z)/k''_*, \;\; k''_* = t_*^2/z_*$, where k'' is the GVD (in units fs^2/mm). In normalized units we find

$$d(z) = \langle d \rangle + \frac{\Delta(z)}{l_c},$$

with $\langle d \rangle$ being the average dispersion (net GVD), Δ the deviation from the average GVD, and l_c the normalized laser-design map length. Usually one considers a two step dispersion map where $\Delta_j, \;\; j = 1, 2$ are taken to be constant in the mirror+prism components ($j = 1$) and crystal ($j = 2$). The map length over which the anomalous dispersion occurs is θl_c where

$0 < \theta < 1$; typically we take $\theta = 1/2$ in Ti:sapphire laser applications. It is convenient to introduce a measure of map strength via the parameter s, which is proportional to the area under the dispersion map, $s = \frac{1}{4}[\theta\,\Delta_1 - (1-\theta)\,\Delta_2]$. In addition to dispersion-management, we also have nonlinear-management in this laser model . Here nonlinear-management means that $n = 1$ (transformed from γ_0 in dimensional variables) inside the Ti:sapphire crystal and $n = 0$ outside the crystal; that is, we assume linear propagation inside the prisms and mirrors.

In our earlier research investigations in fiber optics we derived, based on the asymptotic procedure of multiple scales, a nonlinear integro-differential equation (not given here due to space considerations) which governs the dynamics of dispersion-managed pulse propagation. This governing equation is referred to as the dispersion-managed nonlinear Schrödinger (DMNLS) equation. When there is no gain or loss in the system, for strongly dispersion-managed systems, the DMNLS equation plays the role of the "pure" NLS equation–which is the relevant averaged equation when there is either small or no dispersion-management. When gain and loss are included as in the PES equation we have a modification of the "pure" DMNLS equation.

With or without dispersion-management the PES equation naturally describes the locking and evolution of pulses in mode-locked lasers that are operating in the soliton regime. In our papers typical values of the parameters are chosen, and we vary the gain parameter g and the map strength s. When $g < g^*(s)$ no localized solution is obtained; i.e. in this case the effect of loss is stronger than a critical gain value and the evolution of a Gaussian profile decays to the trivial solution. Conversely, when $g > g^*(s)$, there exists a single localized solution, $u = U_0(t)\exp(i\mu z)$ where μ, called the propagation constant, is uniquely determined given the specific values of the other parameters.

A typical situation is described by the evolution of the pulse peak for different values of the gain parameter g as shown in Fig. 2; here we keep all terms constant and only change

the gain parameter g. When $g = 0.1$ the pulse vanishes quickly due to excessive loss with

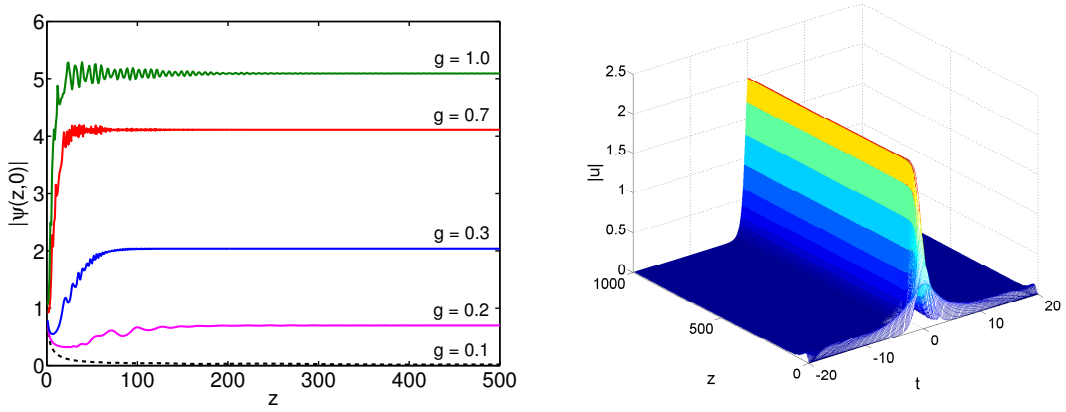

Figure 2: Evolution of the pulse peak of an arbitrary initial profile under PES with different values of gain. The damped pulse-peak evolution is shown with a dashed line. In the right hand figure, the complete evolution is given for $g = 0.3$.

no noticeable oscillatory behavior; the pulse simply decays, resulting in damped evolution. When $g = 0.2, 0.3$, due to the loss in the system the pulse initially undergoes a relative to its amplitude a modest decrease. However, it recovers and evolves into stable solution. Interestingly, e.g. when $g = 0.7, 1$, and the perturbations are not small, a stable evolution is nevertheless again obtained, although somewhat different from the case above. Now with excessive gain in the system, the pulse amplitude increases develops oscillations but a steady state is rapidly reached.

Generally speaking in the PES model, the mode-locking effect is present for $g \geq g^*$, a critical gain value. Without enough gain i.e. $g < g^*$, pulses dissipate to the trivial zero state. Furthermore,we do not find complex radiation states or states whose amplitudes grow without bound for parameter regimes we studied. In terms of solutions, Eq. (1) admits soliton states for all values of $g \geq g^* > l$ (recall, here $l = 0.1$). This was also shown to be the case when we employed analytical methods (soliton perturbation theory).

As the gain parameter increases so does the amplitude and the pulse becomes narrower. The energy and the amplitude of the pulse increases with g. In fact, the energy changes

according to $E \sim \sqrt{\mu}$. Indeed, from soliton theory of the classical NLS equation this is exactly the way a classical soliton's energy changes. The key difference being that in the pure NLS a semi-infinite set of μ exists, whereas now μ is unique for the given set of parameters. Hence one expects that the solutions of the two equations, PES and NLS, are comparable. In Fig. 3 we plot the two solutions for different values of g. In each case the same value of μ is used. The amplitudes match so closely that they are indistinguishable in the figure, meaning the

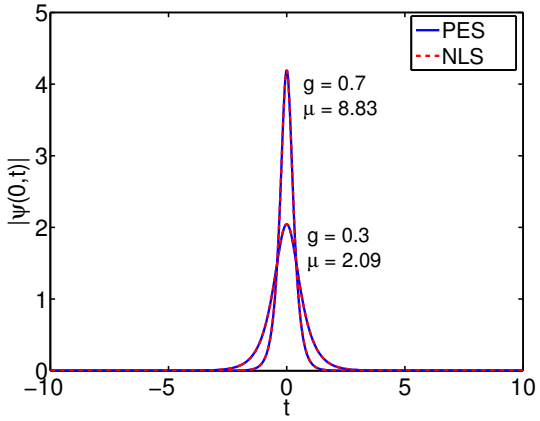

Figure 3: Solitons of the perturbed and unperturbed equations.

perturbing effect is strictly the mode-locking mechanism, i.e. its effect is to mode-lock to a soliton of the pure NLS with the appropriate propagation constant. The solitons of the unperturbed NLS system are well known in closed analytical form, i.e. they are expressed in terms of the hyperbolic secant function, $\psi = \sqrt{2\mu}\,\mathrm{sech}(\sqrt{2\mu}\,t)\exp(-i\mu z)$, and therefore describe solitons of the PES to a good approximation.

It is useful to note that only for a narrow range of parameters does the master laser equation (when the loss term is taken to be the first two terms of the Taylor expansion of the last, power saturated term, in the PES equation) have stable soliton solutions or mode-locking evolution. In general the solitons are found to be unstable; either dispersing to radiation or evolving into nonlocalized quasi-periodic states. For different parameters, the amplitude can also grow rapidly under evolution. Thus, the basic master laser equation

captures some qualitative aspects of pulse propagation in a laser cavity; however, since there is only a small range of the parameter space for which stable mode-locked soliton pulses exist, it does not reflect the wide ranges of operating conditions where mode-locking occurs.

Interestingly, as the gain becomes stronger additional soliton states are possible and 2, 3, 4 or more coupled pulses are found to be supported. This means that strings of soliton states can be obtained. The value of $\Delta\xi/\alpha$, where $\Delta\xi$ and α are the pulse separation and pulse width respectively, is a useful parameter. The full width of half maximum (FWHM) for pulse width is used. $\Delta\xi$, is measured between peak values of two neighboring pulses and $\Delta\phi$ is the phase difference between the peak amplitudes. Using typical parameters, with sufficient gain ($g = 0.5$) Eq. (1) is evolved starting from unit gaussians with initial peak separation $\Delta\xi = 10$ and $\Delta\xi/\alpha = 8.5$. The evolution and final state are depicted in Fig. 4. For the final

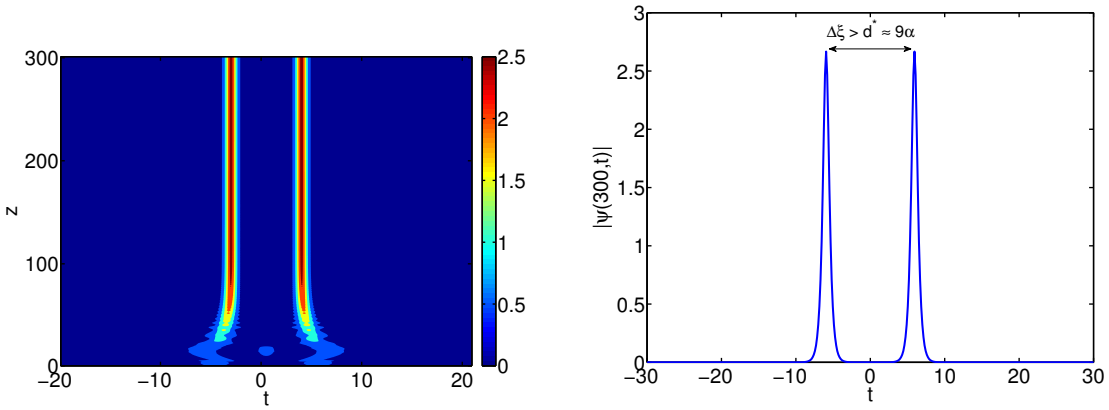

Figure 4: Typical mode-locking evolution (left) for an in phase two soliton state of the anomalously dispersive PES equation and the resulting soliton profile (right) at $z = 300$.

state we find $\Delta\xi/\alpha \approx 10$. As in the single soliton mode-locking case the individual pulses are approximately solutions of the unperturbed NLS equation, namely hyperbolic secants. The pulses differ from a single soliton in that the individual pulse energy is smaller then that observed for the single soliton mode-locking case for the same choice of g, while the total energy of the two soliton state is higher.

In our papers we also investigate the minimum distance, d^*, between the solitons in order

for no interactions to occur over a prescribed distance. We evolve the PES equation starting with two solitons. If the initial two pulses are sufficiently far apart then the propagation evolves to a two soliton state and the resulting pulses have a constant phase difference. If the distance between them is less than a critical value then the two pulses interact in a way characterized by the difference in phase between the peaks amplitudes: $\Delta\phi$. When initial conditions are symmetric (in phase) two pulses are found to merge into a single soliton of Eq. (1). When the initial conditions are anti-symmetric (out of phase by π) then they repel each other until their separation is above this critical distance while retaining the difference in phase, resulting in an effective two pulse high-order soliton state. This does not occur in the pure NLS equation.

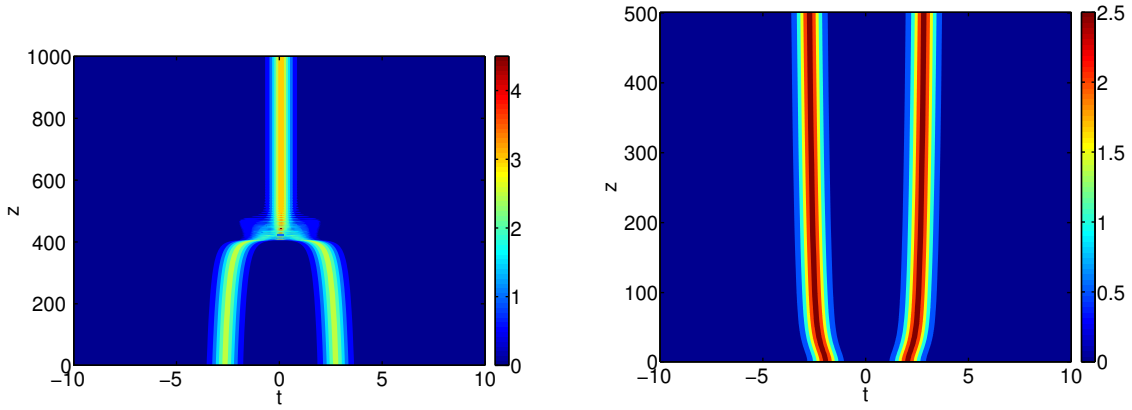

Figure 5: Two pulse interaction when $\Delta\xi < d^*$. Initial pulses ($z = 0$) in phase: $\Delta\phi = 0$, $\Delta\xi/\alpha \approx 7$ (top) merge while those out of phase by $\Delta\phi = \pi$ with $\Delta\xi/\alpha \approx 6$ (bottom) repel.

In the constant dispersion case the critical distance w=for which there is no interaction in a distance $z < z_*$ is found to be $\Delta\xi = d^* \approx 9\alpha$ (see Fig. 4). Interestingly, we remark that this is consistent with the experimental observations. To further illustrate, we plot the evolution of these cases in Fig. 5. At $z = 500$ for the repelling solitons $\Delta\xi/\alpha = 8.9$.

Power saturation models also arise in other problems in nonlinear optics and are central in the underlying theory. For example, power saturation models are important in the study of the dynamics of localized lattice modes (solitons, vortices, etc) propagating in photorefractive

nonlinear crystals. If the nonlinear term in these equations was simply a cubic nonlinearity, without saturation, two dimensional fundamental lattice solitons would be vulnerable to blow up singularity formation, which is not observed. Thus saturable terms are crucial in these problems.

Nonlinear Optics in Waveguide arrays and photonic lattices

Nonlinear light wave propagation in photonic lattices, or periodic optical waveguides, is an active and interesting area of research. This is due, in part, to the realization that photonic lattices can be constructed on extremely small scales, typically a few microns in size. They allow the possibility of manipulation and navigation of lightwaves in small regions. Localized nonlinear optical pulses which occur on one and two dimensional backgrounds have been investigated. These backgrounds can be either fabricated mechanically such as those comprised of AlGaAs materials or all-optically using photo-refractive materials where the photonic structures are constructed via interference of two or more plane waves.

An important dimensionless equation that governs the light propagation in nonlinear inhomogeneous dielectric media is the normalized lattice NLS equation

$$i\psi_z + \nabla^2\psi - V(\mathbf{r})\psi + \sigma|\psi|^2\psi = 0. \tag{2}$$

Here $V(\mathbf{r})$ is an optical potential which describes the transversely varying refractive index; σ is a constant which is positive for focusing nonlinearity and negative for defocusing nonlinearity. The potentials are often periodic, though defects and more complicated potentials have also been studied. In photorefractive crystals, a useful modified model is the normalized saturable lattice NLS equation

$$i\psi_z + \nabla^2\psi - \frac{E_0\psi}{1 + V(\mathbf{r}) + \sigma|\psi|^2\psi} = 0 \tag{3}$$

where E_0 is corresponds to the applied dc field and $\sigma \geq 0$ is the nonlinear coefficient.

Important features of such systems include the existence of multiple frequency gaps of the linear spectra and gap solitons can be obtained in these dispersion band gaps. The linear problem is governed by the classical Schrödinger equation with a potential. If the potential is periodic, this equation and the associated Bloch theory have been well studied in the solid state physics literature. Generally speaking, the above lattice equations omitting nonlinear terms have solutions propagating along z direction, i.e., $\psi(\mathbf{r}, z) = e^{-i\mu z}\varphi(\mathbf{r})$, where $\varphi(\mathbf{r})$ is

the Bloch mode which satisfies

$$\mu\varphi + \nabla^2\varphi - V(\mathbf{r})\varphi = 0. \tag{4}$$

Due to the periodicity of $V(\mathbf{r})$, the Bloch mode $\varphi(\mathbf{r})$ has the form $\varphi(\mathbf{r};\mathbf{k}) = \mathrm{e}^{i\mathbf{k}\cdot\mathbf{r}}U(\mathbf{r};\mathbf{k})$ where $U(\mathbf{r})$ has the same periodicity as the potential $V(\mathbf{r})$; $\mathbf{k}$ is the transverse wave vector and the dispersion surface $\mu(\mathbf{k})$ is periodically dependent on the parameter $\mathbf{k}$ and forms what is referred to as the reciprocal lattice. The unit cell of the reciprocal lattice is called the Brillouin zone and the dispersion surface $\mu(\mathbf{k})$ is defined only in the Brillouin zone. A light beam under propagation is usually a collection of envelopes of the Block modes. So it is important to understand the evolution of such Block mode envelopes.

Periodic structures which have been widely studied are arrays of coupled nonlinear optical waveguides and periodic rectangular lattices. These systems exhibit localized soliton and dipole, multipole modes. In our research papers we find and discuss different phenomena.

Theoretically speaking, all 1-D periodic lattices are essentially the same. However, there can be significant differences between 2-D periodic lattices. A special kind of lattice is the honeycomb (HC) lattice. The local minima of the potentials, called sites, have the index of refraction as maxima and the electric fields are attracted to the sites. The site distribution determines the properties of the lattices. In the HC lattice, there are two sites in one unit cell. The associated dispersion relations have a special property: the first and the second bands touch each other at certain isolated points which are termed Dirac points. The existence of Dirac points allows certain envelopes of the Bloch modes to propagate in an interesting manner–an input spot becomes two expanding bright rings as the beam propagates in the crystal. This phenomenon is called conical diffraction It was first predicted by W. Hamilton in 1832 and observed by H. Lloyd in soon afterwards. Here a narrow beam entering a crystal spreads into a hollow cone within the crystal. The existence of the conical diffraction phenomenon in the light beam propagation in honeycomb lattices was demonstrated both experimentally and numerically by Segev's group. The theoretical explanation was given

in our papers.We find that the envelope evolution is governed by a nonlinear Dirac system. Below we discuss how to derive the nonlinear Dirac system.

We consider 2-D lattices with two periods, i.e. with two independent primitive lattice vectors. We denote $\mathbf{v}_1$ and $\mathbf{v}_2$ as the two lattice vectors and the set of physical lattice vectors with integer translations as $\mathcal{P}$. We also denote $\mathbf{k}_1$ and $\mathbf{k}_2$ as the primitive reciprocal-lattice vectors and $\mathcal{G}$ as the set of reciprocal lattice vectors. The unit cell of the physical lattice Ω is the parallelogram with $\mathbf{v}_1$ and $\mathbf{v}_2$ as its two sides and the unit cell of the reciprocal lattice Ω' is the parallelogram determined by $\mathbf{k}_1$ and $\mathbf{k}_2$. The relation between lattice and reciprocal lattice is $\mathbf{v}_m \cdot \mathbf{k}_n = 2\pi\delta_{mn}$.

An HC lattice is composed of two standard triangular sublattices which we term the A and B sublattices. The A lattice vectors form a triangular lattice. To generate the B sublattice, additional information is needed to determine the shift from the B site to the A site in the same unit cell. We denote this shift as a vector $\mathbf{d}_1$. A typical honeycomb lattice is generated by taking $\mathbf{v}_1 = l\left(\frac{\sqrt{3}}{2}, \frac{1}{2}\right)$, $\mathbf{v}_2 = l\left(\frac{\sqrt{3}}{2}, -\frac{1}{2}\right)$ and $\mathbf{d}_1 = -\frac{1}{3}(\mathbf{v}_1 + \mathbf{v}_2)$. see e.g. Fig. 6. By connecting all the nearest neighbors, an HC lattice is obtained. It is noted that all A sites form a triangular sublattice and all B sites form the other triangular sublattices.

A honeycomb lattice can be constructed from three plane waves, e.g.

$$V(\mathbf{r}) = V_0 \left| \mathrm{e}^{ik_0\mathbf{b}_1\cdot\mathbf{r}} + \mathrm{e}^{ik_0\mathbf{b}_2\cdot\mathbf{r}} + \mathrm{e}^{ik_0\mathbf{b}_3\cdot\mathbf{r}} \right|^2 \tag{5}$$

where $\mathbf{b}_1 = (0, 1)$, $\mathbf{b}_2 = (-\frac{\sqrt{3}}{2}, -\frac{1}{2})$ and $\mathbf{b}_3 = (\frac{\sqrt{3}}{2}, -\frac{1}{2})$; $V_0 > 0$ is the lattice intensity; k_0 is the scaled wave length of the interfering plane waves. The minima of this potential form an HC lattice; the characteristic vectors for this potential are

$$\mathbf{v}_1 = l\left(\frac{\sqrt{3}}{2}, \frac{1}{2}\right), \qquad \mathbf{v}_2 = l\left(\frac{\sqrt{3}}{2}, -\frac{1}{2}\right),$$
$$\mathbf{k}_1 = \frac{4\pi}{\sqrt{3}l}\left(\frac{1}{2}, \frac{\sqrt{3}}{2}\right), \qquad \mathbf{k}_2 = \frac{4\pi}{\sqrt{3}l}\left(\frac{1}{2}, -\frac{\sqrt{3}}{2}\right)$$

where $l = \frac{4\pi}{3k_0}$.

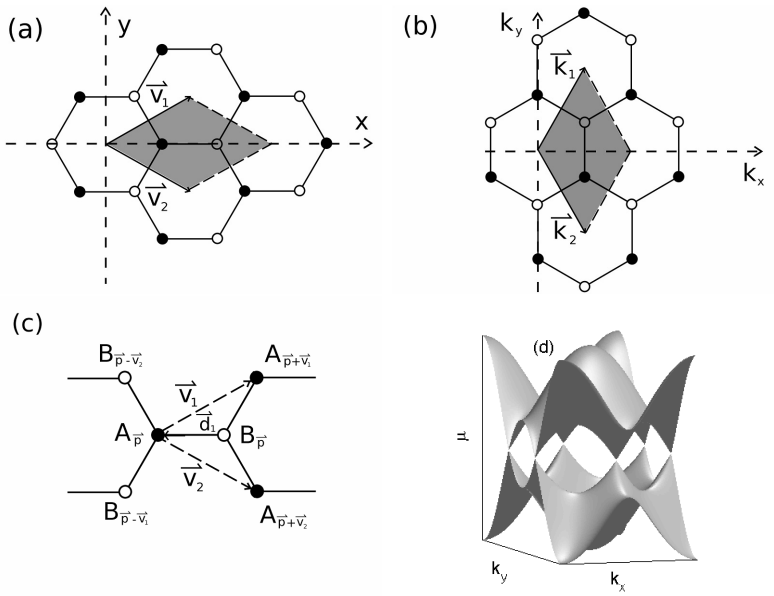

Figure 6: (a) The hexagonal lattice; (b) The reciprocal lattice. Shadow regions are the unite cell Ω and Brillouin zone Ω'. (c) The construction of the A and B sublattices; (d) The dispersion surface.

We consider the lattice NLS equation (2) where σ is small. The above honeycomb lattice potential given by (5) is prototypical.

We next discuss how to derive the dispersion relation and envelope equations the tight-binding limit, i.e., $V_0 \gg 1$. Physically, tight-binding limit means the potential well at each site is very deep, and only on-site and nearest neighbor interactions need to be considered. The potential can be written in the form

$$V(\mathbf{r}) = \sum_{\mathbf{v}} (V_A(\mathbf{r}-\mathbf{v}) + V_B(\mathbf{r}-\mathbf{v}))$$

where V_A, V_B denote the potentials generated from the two sites in the primitive unit cell and they have sharp minima near the A and B sites respectively. Here the sum over $\mathbf{v}$ means $\mathbf{v}$ takes all values in $\mathcal{P}$, i.e., $\mathbf{v} = m\mathbf{v}_1 + n\mathbf{v}_2$, for integers m, n. The Bloch mode is taken to be of the form

$$\varphi(\mathbf{r};\mathbf{k}) = a\sum_{\mathbf{v}} \phi_A(\mathbf{r}-\mathbf{v})\mathrm{e}^{i\mathbf{k}\cdot\mathbf{v}} + b\sum_{\mathbf{v}} \phi_B(\mathbf{r}-\mathbf{v})\mathrm{e}^{i\mathbf{k}\cdot\mathbf{v}} \tag{6}$$

where $\phi_A(\mathbf{r})$ and $\phi_B(\mathbf{r})$ represent an "orbital" (i.e., Wannier function) of a single V_A or V_B

potential respectively. Due to the symmetry, $V_B(\mathbf{r}) = V_A(\mathbf{r} - \mathbf{d}_1)$, so $\phi_B(\mathbf{r}) = \phi_A(\mathbf{r} - \mathbf{d}_1)$ and they have the same eigenvalue denoted as E; i.e.

$$\left(\nabla^2 - V_j(\mathbf{r})\right)\phi_j(\mathbf{r}) = -E\phi_j(\mathbf{r})$$

where j is A or B; Here we only consider the lowest band. We also assume ϕ_A and ϕ_B are real and normalize them with norm 1, i.e., $\int \phi_A\phi_A d\mathbf{r} = \int \phi_B\phi_B d\mathbf{r} = 1$.

Substituting the above Bloch mode $\varphi(\mathbf{r};\mathbf{k})$ into the eigenproblem (4), multiplying by $\phi_j(\mathbf{r})$ and integrating yields a matrix eigenvalue problem. The eigenvalue problem has non-trivial solutions if and only if the determinant is zero which determines the dispersion relation, which has the form

$$\mu(\mathbf{k}) - E = \frac{c_1 \mp c_2|\gamma(\mathbf{k})|}{1 \mp c_0|\gamma(\mathbf{k})|}.$$

where $c_j, j = 1, 2, 3$ are found in terms of integrals over the orbital and potential and

$$\gamma(\mathbf{k}) = (1 + \mathrm{e}^{-i\mathbf{k}\cdot\mathbf{v}_1} + \mathrm{e}^{-i\mathbf{k}\cdot\mathbf{v}_2}).$$

Note that $\gamma(\mathbf{k})$ is periodic over $\mathbf{k}$. In one reciprocal unit cell, there are two zeros of $\gamma(\mathbf{k})$, which we denote K and K'. These are the Dirac points. For the potential (5), in the primitive reciprocal unit cell Ω' (see Fig. 6 (b)), $K = \frac{4\pi}{3l}(\frac{\sqrt{3}}{2}, -\frac{1}{2})$ and $K' = \frac{4\pi}{3l}(\frac{\sqrt{3}}{2}, \frac{1}{2})$. All the zeros of $\gamma(\mathbf{k})$ form the reciprocal hexagonal lattice. At these points $\mu(\mathbf{k})$ has a multiple root. Thus, a and b are free and the associated original linear Schrödinger eigenvalue problem exhibits degeneracy. The upper dispersion surface and the lower dispersion surface touch each other at the zeros of $\gamma(\mathbf{k})$ (see Fig. 6 (d)); at the Dirac points, the eigenvalue problem (4) has two independent Bloch modes.

Now suppose we input a Bloch wave envelope is input into the crystal. To the leading order we assume the envelope varies slowly along z,

$$\psi \sim \left(\sum_{\mathbf{v}} a_{\mathbf{v}}(Z)\phi_A(\mathbf{r} - \mathbf{v})\mathrm{e}^{i\mathbf{k}\cdot\mathbf{v}} + \sum_{\mathbf{v}} b_{\mathbf{v}}(Z)\phi_B(\mathbf{r} - \mathbf{v})\mathrm{e}^{i\mathbf{k}\cdot\mathbf{v}}\right)\mathrm{e}^{-i\mu z}. \tag{7}$$

Since ψ is not a Bloch mode anymore, the intensities are different at different sites, i.e., a and b have subindex $\mathbf{v}$. And $Z = \varepsilon z$ (small parameter ε will be determined later).

Substituting the envelope (7) into the lattice NLS equation, multiplying $\phi_j(\mathbf{r}-\mathbf{p})\mathrm{e}^{-i\mathbf{k}\cdot\mathbf{p}}$ where $\mathbf{p} \in \mathcal{P}$,and integrating we find

$$\begin{aligned}
\varepsilon i\frac{da_{\mathbf{p}}}{dZ} + (\mu - E - c_1)a_{\mathbf{p}} + ((\mu-E)c_0 - c_2)\mathcal{L}_1 b_{\mathbf{p}} + \sigma g|a_{\mathbf{p}}|^2 a_{\mathbf{p}} = 0 \\
\varepsilon i\frac{db_{\mathbf{p}}}{dZ} + (\mu - E - c_1)a_{\mathbf{p}} + ((\mu-E)c_0 - c_2)\mathcal{L}_2 a_{\mathbf{p}} + \sigma g|b_{\mathbf{p}}|^2 b_{\mathbf{p}} = 0
\end{aligned}$$

where

$$\mathcal{L}_1 b_{\mathbf{p}} = b_{\mathbf{p}} + b_{\mathbf{p}-\mathbf{v}_1}\mathrm{e}^{-i\mathbf{k}\cdot\mathbf{v}_1} + b_{\mathbf{p}-\mathbf{v}_2}\mathrm{e}^{-i\mathbf{k}\cdot\mathbf{v}_2},$$

$$\mathcal{L}_2 a_{\mathbf{p}} = a_{\mathbf{p}} + a_{\mathbf{p}+\mathbf{v}_1}\mathrm{e}^{i\mathbf{k}\cdot\mathbf{v}_1} + a_{\mathbf{p}+\mathbf{v}_2}\mathrm{e}^{i\mathbf{k}\cdot\mathbf{v}_2},$$

and $g = \int \phi_A^4 d\mathbf{r} = \int \phi_B^4 d\mathbf{r}$.

We are interested in the envelope of the Bloch mode near Dirac points, so we take for example $\mathbf{k}$ near K. At this point, we find after rescaling,

$$i\frac{da_{\mathbf{g}}}{dZ} - \mathcal{L}_1 b_{\mathbf{p}} + s(\sigma)|a_{\mathbf{p}}|^2 a_{\mathbf{p}} = 0; \tag{8}$$

$$i\frac{db_{\mathbf{g}}}{dZ} - \mathcal{L}_2 a_{\mathbf{p}} + s(\sigma)|b_{\mathbf{p}}|^2 b_{\mathbf{p}} = 0; \tag{9}$$

where we have taken $|\varepsilon| \sim O(c_2) \sim O(|\sigma|)$ to ensure maximal balance and $s(\sigma)$ is the sign of σ or zero if there is no nonlinearity. The above system (8)-(9) is the discrete nonlinear Dirac system.

Next consider a further limit; assume the lattice constant l is much smaller than the characteristic scale of the envelope ρ, i.e., $l \ll \rho$. Then after some calculation, $\mathcal{L}_1 \approx \frac{\sqrt{3}l}{2\rho}(\partial_X + i\partial_Y)$ and $\mathcal{L}_2 \approx \frac{\sqrt{3}l}{2\rho}(-\partial_X + i\partial_Y)$. Here we use X and Y to measure the wide envelopes. Then the discrete system becomes the following continuous system (after rescaling)

$$i\frac{da}{dZ} - (\partial_X - i\partial_Y)b + s(\sigma)|a|^2 a = 0; \tag{10}$$

$$i\frac{db}{dZ} - (-\partial_X - i\partial_Y)a + s(\sigma)|b|^2 b = 0, \tag{11}$$

where we have taken $|\varepsilon| \sim O(c_2 \frac{l}{\rho}) \sim O(|\sigma|)$ to ensure the maximal balance in the continuous problem. Thus, we find the continuous nonlinear Dirac system which governs the envelopes of Bloch modes propagating in the honeycomb lattice. If the envelope is not sufficiently wide, e.g. no transverse slow modulation, the discrete system is required to describe the envelope evolution. If the envelope is very wide, the continuous systems is sufficient.

Here we use the continuous Dirac system to describe typical conical diffraction. We compare the numerical simulations of both lattice NLS equation and the nonlinear Dirac system. The comparison is displayed in Fig. 7. is from the lattice NLS equation (2) with initial conditions being a Bloch mode multiplied a wide Gaussian. Note that we can see the background fine lattice structure. The bottom panel is from the nonlinear Dirac system (10)-(11). Initially, a is a unit Gaussian and b is zero. From the top panel we see that a spot becomes two rings which separated by a dark ring. The simulation of the nonlinear Dirac system gives excellent correspondence.

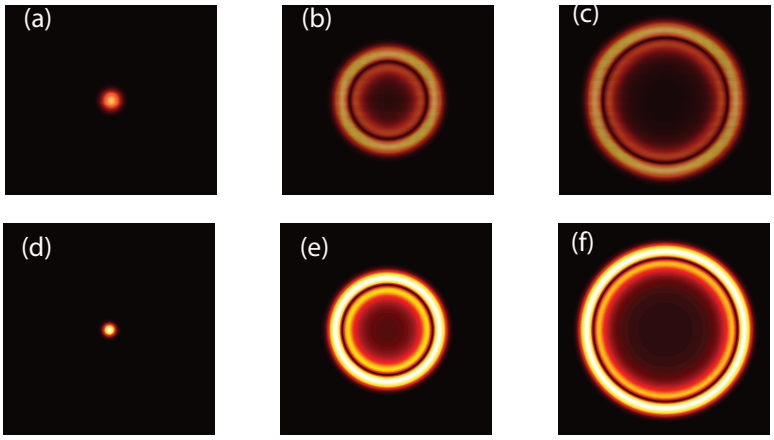

Figure 7: The propagation of a Gaussian Bloch mode envelope associated with a Dirac point. Top: simulations of the lattice NLS equation (2); Bottom: simulations of the nonlinear Dirac Eqs.(10) and (11). Here only a envelope is displayed.

In recent work we have studied stronger nonlinear cases and have found that either the above discrete Dirac system is needed or we must keep higher order terms in our asymptotic analysis.

Similarly we have studied a different case, one where the honeycomb potential is weak or 'shallow'; i.e. $\delta \sim |V| \ll 1$. In this case we find the underlying dispersion relation has triple degeneracy at leading order in δ and double degeneracy at higher orders. These degenerate points correspond to the Dirac points in the shallow potential limit. Slowly varying envelope equations were also obtained in various limits depending on the envelope scale as compared with the size of nonlinearity. In these cases we find underlying Dirac type nonlinear envelope systems.

Dark Solitons

Dark solitons, namely envelope solitons having the form of density dips with a phase jump across their density minimum, are fundamental nonlinear excitations which arise, for example, in the defocusing nonlinear Schrödinger (NLS) equation. They are termed *black* if the density minimum is zero or *grey* otherwise. The discovery of these structures, which dates back to early 70's, was followed by intensive study both in theory and in experiment: in fact, the emergence of dark solitons on a modulationally stable background is a fundamental phenomenon arising in diverse physical settings. Indeed, dark solitons have been observed and studied in numerous contexts including: discrete mechanical systems electrical lattices, magnetic films, plasmas, fluids, atomic Bose-Einstein condensates as well as nonlinear optics.

In nonlinear optics, dark solitons are predicted to have some advantages as compared to their bright counterparts (which are supported by the focusing NLS model): dark solitons can be generated by a thresholdless process, they are less affected by loss, and background noise, they are more robust against Gordon-Haus jitter and higher order dispersion etc.

Recently, there has been an interest in "dark pulse lasers", namely laser systems emitting trains of dark solitons on top of the continuous wave (cw) emitted by the laser; various experimental results have been reported utilizing fiber ring lasers, quantum dot diode lasers and dual Brillouin fiber lasers. These works, apart from introducing a method for a systematic and controllable generation of dark solitons, can potentially lead to other important applications related, e.g., with optical frequency combs, optical atomic clocks, and others. An important aspect in these studies is the ability of the laser system to induce a fixed phase relationship between the modes of the laser's resonant cavity, i.e., to *mode-lock*; in such a case, interference between the laser modes in the normal dispersion regime causes the formation of a sequence of dark pulses on top of the stable cw background emitted by the laser.

We have studied dark solitons subject to general perturbations

$$iu_z - \frac{1}{2}u_{tt} + |u|^2 u = F[u] \tag{12}$$

where $F \ll 1$ and in mode-locked (ML) lasers. As a prototypical example, we considered the perturbation theory within the framework of the PES equation (see earlier discussion) in the normal regime. In this case using the PSE model, $F[u]$ is expressed in the following dimensionless form:

$$F[u] = \frac{ig}{1 + E/E_{\text{sat}}}u + \frac{i\tau}{1 + E/E_{\text{sat}}}u_{tt} - \frac{il}{1 + P/P_{\text{sat}}}u, \tag{13}$$

In terms of optics applications, $u(z,t)$ is the complex electric field envelope, z the direction of propagation and t retarded time. We consider the boundary conditions $|u(z,t)| \to u_\infty(z)$ as $|t| \to \infty$. In the PES equation, P and E represent the power and energy of the system, while P_{sat} and E_{sat} denote corresponding saturation values, respectively; g, τ, and l are positive real constants, with the corresponding terms representing gain, spectral filtering (both saturated with energy), and loss (saturated with power).

Our analysis shows that, in general, perturbations of dark solitons induce a small but wide shelf. We can calculate the perturbation to the soliton parameters as well as the shelf. Under certain perturbations, the Korteweg-deVries equation also exhibits shelf phenomena. In a ring like laser system the PES model has rather pronounced shelf characteristics. In Figure (8) below, a typical situation is depicted for a ring laser system described by the PES equation. The shelf is seen to be prominent in the PES equation. No shelf exists in the unperturbed NLS equation. In the inset of the figure the phase change across the dark soliton is given for the PES model vs. the unperturbed NLS equation.

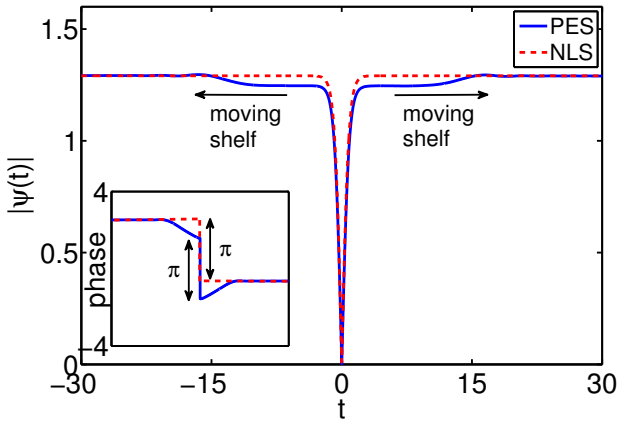

Figure 8: The development of a shelf in the solution to the PES equation in a ring laser configuration (solid line) as compared to the solution of the NLS equation (dashed line). The shelf is evident in the amplitude. The inset shows how the phase changes across the soliton.

Dispersive Shock Waves

Shock waves in compressible fluids is a classically important field in applied mathematics and physics, whose origins date back to the work of Riemann. Such shock waves, which we refer to as classical or viscous shock waves (VSW's), are characterized by a localized steep gradient in fluid properties across the shock front. Without viscosity one has a mathematical discontinuity; when viscosity is added to the equations, the discontinuity is "regularized" and the solution is smooth. An equation that models classical shock wave phenomena is the Burgers equation

$$u_t + uu_x = \nu u_{xx} \tag{14}$$

If $\nu = 0$, we have the inviscid Burgers equation which admits wave breaking. When the underlying characteristics cross a discontinuous solution, i.e. a shock wave, is introduced which satisfies the Rankine-Hugoniot jump conditions which, in turn, determines the shock speed. Analysis of Burgers equation shows that there is a smooth solution given by

$$u = \frac{1}{2} - \frac{1}{2}\tanh\{\frac{1}{4\nu}(x - \frac{1}{2}t)\}$$

which tends to the shock solution as $\nu \to 0$. Thus the mathematical discontinuity is regularized when viscosity ν is introduced.

Another type of shock wave is a so-called dispersive shock wave (DSW). Early observations of DSW's were ion-acoustic waves in plasma physics. Subsequently, Gurevich and Pitaevskii studied the small dispersion limit of the Korteweg-deVries (KdV) equation. They obtained an analytical representation of a DSW. As opposed to a localized shock as in the viscous problem, the description of a DSW is one with a sharp front with an expanding, rapidly oscillating rear tail. The Korteweg-deVries (KdV) equation with small dispersion is given by

$$u_t + uu_x = \epsilon^2 u_{xxx} \tag{15}$$

where $|\epsilon| \ll 1$ regularizes the discontinuity that otherwise would be present. The mathematical technique used to analyze DSW's relies on wave averaging, often referred to as Whitham theory. Whitham theory is used to construct equations for the parameters associated with slowly varying wavetrains; it provides an analytical basis for DSW dynamics. For KdV the Whitham equations can be transformed into Riemann-invariant form, which can be analyzed in detail. One finds that there are two speeds associated with a DSW: one is the speed associated with the frontal wave which is a soliton (located at x_s in the figure), and the other speed corresponds to the group velocity of near linear trailing waves on the rear end (depicted by x_l in the figure) of the DSW. The picture and details are quite different from viscous shock waves which, for example, occurs in Burgers equation; see Fig. 9 left, which depicts a typical DSW associated with the KdV equation and a classical or viscous shock wave (located at x_c in the figure) associated with the Burgers equation. Interestingly, the structure of the KdV DSW is strikingly similar to the original plasma observations.

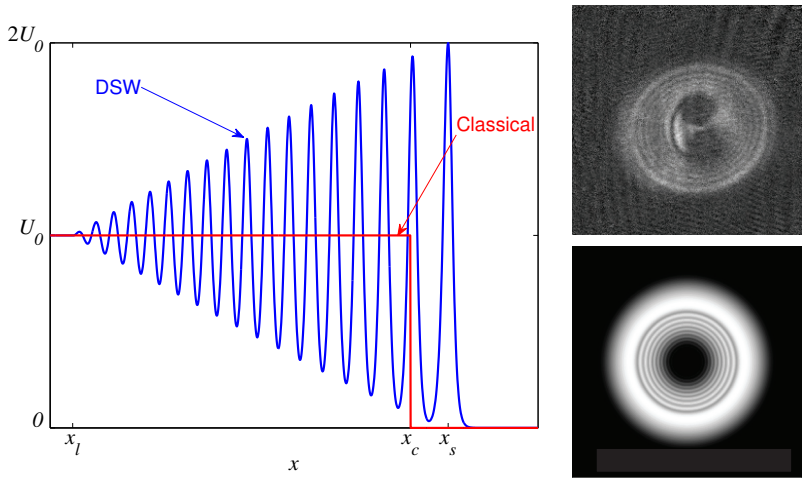

Figure 9: Left figure: typical DSW satisfying the KdV eq. (15) and a classical shock wave satisfying Burgers eq. (14); right figure: typical blast wave–experiment; numerical simulation is given below the experiment.

Recent experiments in Bose-Einstein condensates (BEC) and nonlinear optics have enhanced interest in DSW's. The BEC experiments, originally performed in the Physics De-

partment at the University of Colorado, motivated our studies. The dispersive blast wave experiment and computational results are shown Fig. 9 – middle and right figures. Recent experiments in nonlinear optics carried out in the laboratory of J. Fleischer at Princeton University have also observed similar blast waves and other interesting DSW phenomena.

The governing equations we studied are a defocusing NLS equation with an additional external potential. In BEC this equation is usually called the Gross-Pitaevski equation. Importantly, a similar equation occurs in nonlinear optics. The equation is given in normalized form as

$$i\epsilon\Psi_t + \frac{\epsilon^2}{2}\nabla^2\Psi - V(r,z,t)\Psi - |\Psi|^2\Psi = 0 \tag{16}$$

where $V(r,z)$ contains details describing the cylindrically symmetric potential trap and additional laser terms, Ψ is the wavefunction and ϵ^2 is a small parameter related to the condensate. Two different configurations were studied: the so-called "in-trap" and "out-of-trap" cases. The BEC blast wave in the figure corresponds to a tightly focused laser beam impinging on the BEC in a trapped or an expansion configuration. The laser beam creates a dispersive blast wave in the radial direction.

Numerical simulations were found to agree extremely well with the experiments. In Fig. 9 (right figure), typical experimental and numerical results for a trapped configuration are shown; the numerical image is a contour plot of $\int |\Psi|^2 dz$ (darker is less dense).

Our initial analytical studies for the BEC were carried out on the 1-D semi-classical NLS equation without the external potential since the experiments indicated that after some propagation time the DSW's were approximately 1-D in character and weakly influenced by the potential. Our analytical approach to DSW's uses Whitham averaging theory. Whitham analysis associated with NLS equations in various contexts have been investigated by a number of authors and in order to effectively compare the analysis with BEC experiment and simulations, by ourselves.

Whitham averaging over the first four conservation laws of NLS, using a 1-phase traveling

wave solution, leads to suitable parameters satisfying a system of hyperbolic PDE's which can be written in Riemann-invariant form. Solving the Riemann-invariant system corresponding to step initial data, yields a description of an NLS DSW. The NLS DSW is a slowly modulated wave train which varies from a large trailing wave which is well approximated by a moving dark (grey) soliton, to a nearly linear wavetrain at the front moving with its group velocity; like KdV the NLS DSW has two speeds. The 1-D NLS theory was also applied to the multi-dimensional blast wave cases. The analytical results were very good; however due to radial and potential effects there is a difference in phase and to a lessor degree in amplitude.

While interactions of viscous shock waves are well known, the situation associated with interacting DSW's is still at an early stage. Nevertheless have made some progress; research is continuing in order to develop a broad and detailed understanding. We are investigating DSW interactions in physically interesting systems by employing both Whitham methods and asymptotic analysis applied to the solution obtained by the inverse scattering transform. We note that in recent nonlinear optics experiments carried out in J. Fleischer's laboratory, interacting DSW's were observed.

Dispersive shock waves are an interesting and developing area of research which we believe will play an increasingly important role in nonlinear optics applications and other areas of physics.

PERSONNEL SUPPORTED

- Faculty: Mark J. Ablowitz
- Post-Doctoral Associates: T. Horikis, Y. Zhu
- Other (please list role) None

PUBLICATIONS

- **ACCEPTED/PUBLISHED**
- **Books/Book Chapters**

1. Nonlinear Dispersive Waves, Asymptotic analysis and Soltions, M.J. Ablowitz, Cambridge University Press, Cambridge, UK, 2011.

- **Conference Proceedings–refereed**

1. Nonlinear waves in optics and fluid dynamics, Mark. J. Ablowitz, Proceedings of the International conference on numerical analysis and applied mathematics, (2009).

- **Journals**

1. Asymptotic Analysis of Pulse Dynamics in Mode-locked Lasers, Mark J. Ablowitz, Theodoros P. Horikis, Sean D. Nixon and Yi Zhu, *Stud. Appl. Math.* **122** (2009) 411-425.

2. Conical Diffraction in Honeycomb lattices, Mark J. Ablowitz, Sean D. Nixon and Yi Zhu, *Physical Review A*, **79** (2009) 053830.

3. Soliton Generation and Multiple Phases in Dispersive Shock and Rarefaction Wave Interaction, M. J. Ablowitz, D.E. Baldwin, and M. A. Hoefer, *Physical Review E*, **80** (2009) 016603.

4. Solitons and spectral renormalization methods in nonlinear optics, M. J. Ablowitz and T. P. Horikis, *Eur. Phys. J. Special Topics* **173** (2009) 147-166.

5. Solitons in normally dispersive mode-locked lasers, M.J. Ablowitz and T.P. Horikis, *Physical Review A* **79** (2009) 063845.

6. Soliton strings and interactions in mode-locked lasers, Mark J. Ablowitz, Theodoros P. Horikis and Sean D. Nixon *Opt. Commun.***282** (2009) 4127-4135.

7. Nonlinear waves in optical media, Mark J. Ablowitz, Theodoros P. Horikis, *Journal of Computational and Applied Mathematics* **234** (2010) 1896-1903.

8. Band Gap Boundaries and Fundamental Solitons in Complex 2D Nonlinear Lattices, M.J. Ablowitz, N. Antar, I. Bakirtas and B. Ilan, *Physical Review A*, **81** (2010) 033834.

9. Evolution of Bloch-mode-envelopes in two-dimensional generalized honeycomb lattices, Mark J. Ablowitz, and Yi Zhu, *Physical Review A* **82** (2010) 013840.

10. Perturbations of dark solitons, M. J. Ablowitz, S. D. Nixon, T. P. Horikis and D. J. Frantzeskakis, *Proc. Roy. Soc. A* **467** (2011) 2597-2621.

11. Nonlinear wave dynamics: from lasers to fluids, Mark J. Ablowitz, Terry S. Haut, Theodoros P. Horikis, Sean D. Nixon and Yi Zhu, *Discrete and Continuous Dynamical Systems* **4** (2011) 923-955

12. Dark solitons in mode-locked lasers, M. J. Ablowitz, T. P. Horikis, S. D. Nixon, and D. J. Frantzeskakis, *Opt. Lett.* **36** (2011) 793-795.

13. Nonlinear diffraction in photonic graphene, Mark J. Ablowitz, and Yi Zhu, *Opt. Lett.* **36** (2011) 3762-3764.

14. Nonlinear waves in shallow honeycomb lattices, M. J. Ablowitz and Yi Zhu, Accepted, SIAM Journal on Applied Mathematics (2011)

- **Conferences, Seminars**

- **INTERACTIONS/TRANSITIONS**

1. Distinguished Research Lecture, University of Colorado, Boulder, April 3, 2009, "Extraordinary waves and math–from beaches to lasers".

2. Department of Physics University of Rome III, 12 hour short-course on "Nonlinear Waves and Solitons": April 27-May 5, 2009.

3. Department of Physics University of Rome III, "Nonlinear waves in optics and fluid dynamics", May 6, 2009.

4. Department of Mathematics University of Perugia, "Nonlinear waves in optics and fluid dynamics", May 7, 2009.

5. International Conference, on Analysis and Computation, June 24-28, Shanghai China, Shanghai Normal Univ., "Nonlinear waves in optics and fluid dynamics", June 24, 2009.

6. Department of Mathematics, University of Washington, "Solitary waves: from optics to fluid dynamics", December 5, 2006

7. SIAM annual Meeting July 6-10, 2009, Denver, CO, Special session: Mode-locked lasers, "Pulses, properties and dynamics in mode locked lasers", July 9, 2009.

8. AFOSR Workshop: Nonlinear Optics, Dayton Ohio, September 9-10, 2009, "Pulses, properties and dynamics of mode locked lasers", September 9, 2009

9. International Conference on numerical analysis and applied mathematics, Rythymnon, Crete, Greece, Sept. 18-23, 2009, "Nonlinear waves in optics and fluid dynamics", Sept. 20, 2009,

10. Department of Physics University of Athens, Athens, Greece, "Extraordinary waves –from beaches to lasers", Sept. 24, 2009.

11. Department of Mathematics, University of Colorado Colorado Springs, First Annual Distinguished Lecture, "Extraordinary waves: from beaches to lasers", Oct. 8, 2009.

12. Southeastern SIAM conference, Department of Mathematics, North Carolina State University, March 20-21, 2010, "Nonlinear waves–from beaches to lasers", March 20, 2010

13. Department of Mathematics, University of Saskatchewan, Saskatoon, Canada, "Nonlinear waves–from beaches to lasers", March 23, 2010

14. International Conference: Frontiers in Nonlinear Waves in honor of V.E. Zakharov, Department of Mathematics, University of Arizona, Tucson, AZ, "Nonlinear waves–from beaches to lasers", March 27, 2010.

15. Department of Mathematics, University of New Mexico, Albuquerque, NM "Nonlinear waves–from beaches to lasers", April 8, 2010.

16. International Conference: Symmetries Plus Integrability in honor of Y. Kodama, June 10-14, "A nonlinear waves world: from beaches to lasers", June 10, 2010.

17. International Workshop on Nonlinear Optics, Nankai University, Tianjin, China, "Nonlinear waves–from beaches to lasers", June 30, 2010.

18. AFOSR Workshop: Nonlinear Optics, Albuquerque, NM, Sept 21-22, 2010, "Evolution of Nonlinear Wave Envelopes in Photonic Lattices", Sept. 21, 2010

19. JILA Colloquium, Univ. of Colorado, Boulder, Nov 2, 2010, "All About Waves"

20. Seventh International Conference on Differential Equations and , Dynamical Systems, Univ. South Florida, Dec. 15-18, 2010; "Nonlinear waves–from beaches to lasers", Dec. 15, 2010

21. Dept. of Electrical and Computer Engineering, Univ. of Colorado, Boulder, COSI Seminar Series, "Nonlinear waves–from beaches to lasers", Jan. 24, 2011

22. International Conference on 'Integrability and Physics'–in Honor of A. Degasperis 70th birthday; Dept of Physics Univ of Rome, Italy, Nonlinear Waves in Photonic Lattices and "Optical Graphene", March 25, 2011

23. Dept. of Physical Chemistry, Scuola Normale, Pisa, Italy, "Nonlinear waves–from beaches to Optical Graphene", March 29, 2011

24. Conference on Nonlinear Waves, Univ of Georgia, Athens Georgia, April 3-6, 2011, "Nonlinear waves–from beaches to Photonic Graphene", April 3, 2011

25. Dept. of Applied Mathematics, Columbia Univ, April 13-16, 2011, "Nonlinear waves–from beaches to Optical Graphene", April 15, 2010

26. Invited member: 'SQuaRE: Nonlinear wave equations; American Institute of Mathematics (AIM), May 9-14, 2011

27. Conference on Nonlinearity and Coherent Structures, Univ. of Reading, July 6-8, 2011, Distinguished IMA lecturer, "Nonlinear waves–from beaches to Optical Graphene", July 9, 2011

28. Physics Department, University of Colorado, Boulder, Aug. 31, 2011, "What you always wanted to know about nonlinear waves but..."

29. International Conference on Scientific Computing, Pula, Sardinia, Italy - October 10-14, 2011, "Nonlinear waves: from oceans to optical graphene", Oct 11, 2011

30. AFOSR Workshop: Nonlinear Optics, Albuquerque, NM, Oct 18-19 2011, "Nonlinear Waves in Photonic Lattices and 'Optical Graphene", Oct 19, 2011

31. Joint American-South African Mathematics Society International Mathematics Conference, Nov 29-Dec 2, 2011, "Nonlinear Waves' and Applications"

- **Consultative and Advisory Functions to Other Laboratories and Agencies:** None

- **Transitions:** none

NEW DISCOVERIES, INVENTIONS, OR PATENT DISCLOSURES: None

HONORS/AWARDS:

- Named as one of the most highly cited people in the field of Mathematics by the ISI Web of Science, 2003-present

- Distinguished Research Lecturer (including 1-yr. fellowship), Univ. of Colorado, Boulder, 2009

- Named SIAM (Society of Industrial and Applied Mathematics) Fellow 2011–